(25) Gibbs, J. H.; Adam, G. J. *J. Chem. Phys.* **1965**, *43*, 139-146.
(26) Cheradame, H. In *IUPAC Macromolecules*; Benoit, H., Rempp, P., Eds.; Pergamon: New York, 1982; pp 251-264.
(27) (a) Marcus, Y. *Ion Solvation*; Wiley: New York, 1985; pp 180-184. (b) Davies, C. W. *Ion Association*; Butterworths: Washington, 1962; pp 150-161. (c) Irish, D. E. In *Physical Chemistry of Organic Solvent Systems*; Covington, A. K., Dickinson, T., Eds.; Plenum: New York, 1973; pp 433-460.
(28) Papke, B. L.; Ratner, M. A.; Shriver, D. F. *J. Electrochem. Soc.* **1982**, *129*, 1434-1438.
(29) MacCallum, J. R.; Tomlin, A. S.; Vincent, C. A. *Eur. Polym. J.* **1986**, *22*, 787-791.
(30) Turnbill, D.; Cohen, M. H. *J. Chem. Phys.* **1970**, *52*, 3038-3041.
(31) Spiro, M. In *Physical Methods of Chemistry*; Rossiter, B. W., Hamilton, J. E., Eds.; Wiley: New York, 1986; Vol. 2, pp 663-791.
(32) Watanabe, M.; Sanui, K.; Ogata, N.; Inouye, F.; Kobayashi, T.; Ohtiki, Z. *Polym. J.* **1985**, *17*, 549-555.
(33) Jansen, M. L.; Yeager, H. L. *J. Phys. Chem.* **1973**, *26*, 3089-3092.

Phase Relationships and Conductivity of the Polymer Electrolytes Poly(ethylene oxide)/Lithium Tetrafluoroborate and Poly(ethylene oxide)/Lithium Trifluoromethanesulfonate

S. M. Zahurak,* M. L. Kaplan, E. A. Rietman, D. W. Murphy, and R. J. Cava

AT&T Bell Laboratories, Murray Hill, New Jersey 07974. *Received July 8, 1987*

ABSTRACT: Solid polymer electrolytes are potentially useful in all solid-state rechargeable batteries because of their elastic properties that allow for reduced interfacial contact resistance between the electrolyte and electrodes as well as for thin-film configurations. In this work a study of the complexes of poly(ethylene oxide) with two different salts, $LiBF_4$ and $LiCF_3SO_3$, is presented. As a result pseudobinary pseudoequilibrium phase diagrams (PPD) have been constructed that provide an improved basis for understanding the mechanism of ionic transport. Differential scanning calorimetry and X-ray diffraction have been used to collect data necessary for the PPD. A single-phase crystalline complex over the stoichiometries between 4:1 (monomer/salt) and 3:1 has been established in the case of the BF_4 salt. The $PEO_8(LiBF_4)$ sample exhibited the highest conductivity (9×10^{-4} S/cm) with an activation energy of 0.27 eV. The $LiCF_3SO_3$ complex was unusual in that evidence for a second complex (7:1) was obtained in addition to the more commonly observed 3.5:1 phase. These results were compared to phase diagrams published by others for the same and similar systems.

Since the discovery of fast alkali ion conductivity in polymer salt complexes (conductivity $>10^{-5}$ S/cm at 80 °C)[1] researchers have been avidly seeking a solid polymeric electrolyte (SPE) that would solve the chemical reactivity problems of lithium anodes with the more commonly used liquid organic and solid electrolytes in batteries. Two simple polymer systems have been studied most extensively, poly(ethylene oxide) [PEO] and poly(propylene oxide) [PPO]. A large number of complexes are formed by these polymers, a list of some of them has been compiled by Armand and co-workers.[2]

Despite studies by many groups, most of which have concentrated on complexes of PEO with salts such as $LiClO_4$ and $LiCF_3SO_3$, the structure and conductivity mechanism remain unclear. This study presents pseudobinary pseudoequilibrium phase diagrams (PPD) that furnish important compositional information and lay the structural groundwork which is crucial for understanding the conductivity processes. The polymer/salt systems cannot be described as true binary systems as in typical alloy phase diagrams because both the polymer (PEO) and the polymer/salt complex each contain crystalline and amorphous phases. In addition, these phases are present in variable amounts depending on temperature which means they are not necessarily at an equilibrium state. Therefore, these diagrams are referred to as pseudophase diagrams (PPD). These data concentrate on two PEO/Li^+ systems and compare conductivity results with PPD information. A comparison is also made between this work and similar efforts by Minier, Berthier, and co-workers, which stresses NMR results.[3] Pseudo phase diagram information has been compiled through differential scanning calorimetry and X-ray diffraction. The $PEO/LiBF_4$ system was chosen as the subject of study for its good total conductivity as found in a survey study of Li^+ conductors at moderate temperatures (10^{-5} S/cm at 60 °C).[4] The other system included here, and on which the majority of studies to date has concentrated, is $PEO/LiCF_3SO_3$. This polymer/salt combination has been shown to offer good electrochemical stability as well as promising ionic conductivity.[5]

Experimental Section

The source of PEO was the Aldrich Chemical Co. and had a molecular weight of 5×10^6. The $LiBF_4$ used was supplied and analyzed by Lithium Corp. of America showing 0.03% water content. This was additionally dried at 50 °C under vacuum prior to use. $LiCF_3SO_3$ was prepared by reaction of Li_2CO_3 and CF_3SO_3H (trifluoromethanesulfonic acid) in water. The product was dried by warming under a flow of dry nitrogen and recrystallized from an acetonitrile/toluene mixture. The final product was dried in vacuum at 110 °C. The IR spectrum was essentially identical with that of commercial material. All operations performed by using the polymer and salt were done in a dry, inert atmosphere to eliminate water contamination which has been shown to have a significant effect on conductivity measurements.[6] The solids were weighed in a drybox and mixed together with distilled acetonitrile (approximately 1 g of polymer to 50 mL of solvent). Mixtures were stirred in the drybox for ~36 h. Acetonitrile was distilled from anhydrous potassium carbonate and transferred under dry nitrogen to the glovebox before use. Mixtures of (moles of PEO monomer):(moles of Li salt) were prepared ranging from 2:1 to 40:1 for $LiBF_4$ and 25:1 to 1:1 for $LiCF_3SO_3$. Films of the complexes were cast, on a ~500-mg scale on a PTFE plate mold, by permitting the solvent to evaporate in the glovebox at room temperature for 2 days. IR monitoring for residual solvent or H_2O in the films was negative after this time period.

A Du Pont 1090 thermal analyzer was used to perform calorimetry. Samples were prepared in the drybox by cutting pieces of the film into small squares to fit into a hermetically sealed aluminum pan. The temperature scale was calibrated by using a Na standard. Transition temperatures were specified by the

0024-9297/88/2221-0654$01.50/0

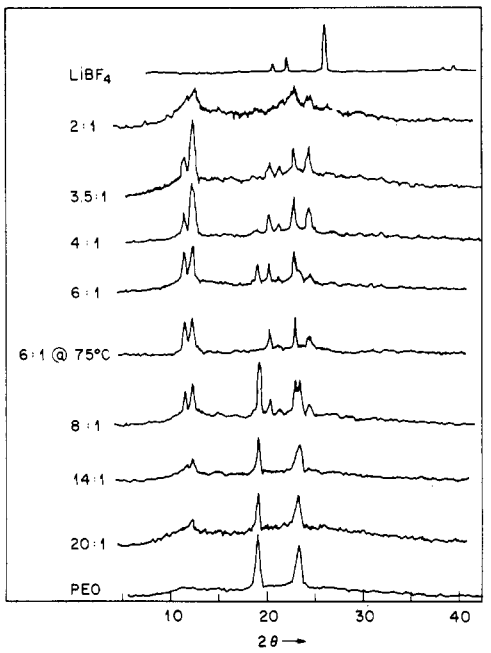

Figure 1. X-ray diffraction patterns of several representative compositions in the $PEO_x(LiBF_4)$ system, including pure PEO and pure $LiBF_4$ (Cu Kα radiation).

endothermic peak maxima. Data were taken at a 10 °C/min heating rate through the temperature range −120 to 220 °C, under a nitrogen purge, with liquid nitrogen as the coolant. Each sample scan was repeated over the same temperature range after slowly cooling (~5 °C/min) to room temperature. Changing scan rates did not significantly alter the appearance of the data.

A Rigaku miniflex diffractometer using Cu Kα radiation was utilized for X-ray diffraction patterns. Polymer film samples were fixed onto a microscope slide with a small amount of silicone grease in the drybox. The slide was mounted in an O-ring sealed brass can with a mylar window to maintain an inert atmosphere.

A Reichert polarizing microscope in combination with a Mettler FP21 hot stage equipped with a dry nitrogen purge was used to identify crystalline and amorphous phase changes. Magnification was limited to 10× with the use of the hot stage. Polymer film samples were prepared by cutting ~0.5 cm^2 pieces and hot pressing them between a microscope slide and cover slip. Loss of birefringence was observed as the samples were slowly heated to temperatures corresponding to transition regions found in the DSC data.

Conductivity measurements were made on samples prepared as follows. Within the drybox, film samples were cut into 1 cm^2 pieces and placed in a threaded ceramic die. Flat-faced stainless-steel screw electrodes were inserted into both ends and pressed against the sample with a ~10 kpsi force. The conductivity cell was then removed from the drybox, whereupon wire leads and a thermocouple were attached. The entire assembly was then placed in a dry-nitrogen-purged computer-controlled furnace.

Complex impedance measurements were made every few degrees during heating. At each temperature the system was equilibrated for 30 min. impedance measurements were made from 5 Hz to 13 MHz by using a computer-controlled Hewlett-Packard 4192A impedance analyzer. The dc resistance was determined by the intersection of the electrode characteristic with the real axis in the complex impedance plane plot.

Results and Discussion

Figures 1 and 2 present X-ray data of the series of polymer/salt concentrations prepared for $PEO/LiBF_4$ and $PEO/LiCF_3SO_3$, respectively. Both reflect a progressive change in the diffraction pattern with crystalline PEO peaks losing intensity as more salt is added to the pure polymer. For both salt complexes all traces of free crystalline PEO disappear at the stoichiometry $PEO_{3.5}$ (salt), indicating full complexation of the crystalline PEO. Also at this concentration, reflections arising from free salt are

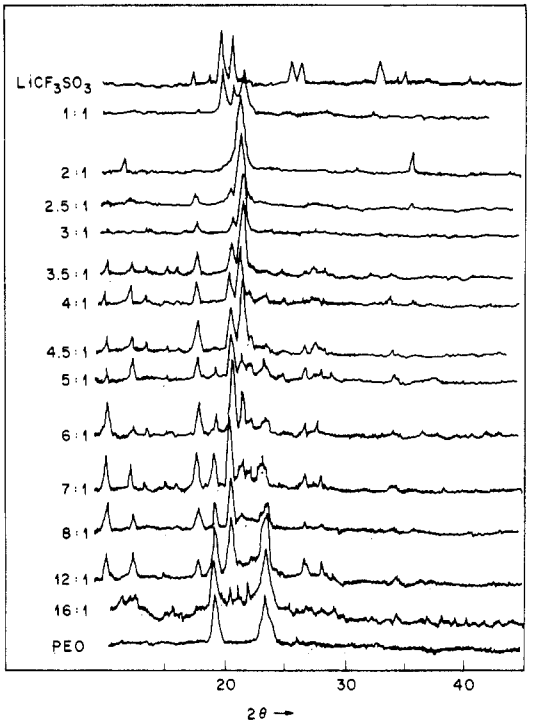

Figure 2. X-ray diffraction patterns similar to Figure 1 for the $PEO_x(LiCF_3SO_3)$ system.

not present in the X-ray pattern. This indicates a single phase crystalline complex at this stoichiometry. For the $PEO/LiBF_4$ system, weak broad reflections from the complex begin appearing even at very low concentrations of $LiBF_4$ (20:1). The crystalline complex diffraction pattern slowly grows in as reflections for the crystalline PEO diminish progressively with additional salt.

The $PEO/LiCF_3SO_3$ system, on the other hand, exhibits a different type of transformation from low salt concentration to high. Here, there is evidence that one phase begins to form at low salt concentrations (25:1), and then as the $LiCF_3SO_3$ concentration increases, the intensity of these lines increases up to about the 7:1 level. At this point the reflections, especially those at 2θ values of 20.53 and 21.45 begin to change relative intensities. By the 4.5:1 level the peak at 21.45 is dominant. The magnitude of this peak continues to increase while at the same time the other reflections diminish. This is clearly characteristic of one phase growing in as another disappears.

At the 2:1 concentration, very little peak intensity remains from the peaks observed in the 7:1 sample pattern. This gradual change in relative intensities implies the presence of another separate crystalline phase in the $PEO/LiCF_3SO_3$ system besides the 3.5:1 complex. The largest reflections for this separate phase are exhibited at the 7:1 concentration. Therefore, from X-ray diffraction data two crystalline complex phases are proposed. The existence of this second phase is justifiable when the crystal structure of the pure uncomplexed polymer is considered.

Takahashi and Tadokoro[7] have established the crystal structure of uncomplexed PEO as four $^7/_2$ helical turns passing through a unit cell with parameters, a = 8.05 Å, b = 13.04 Å, c (fiber axis) = 19.48 Å, and β = 125.4° in the space group $P2_1/a$—C_{2h}^5. It is very easy to envision two separate phases forming, one (at ~3.5:1 phase A) where one Li ion is associated with 3.5 oxygens of a single helix within a polymer matrix of PEO helixes and another (phase B) with the Li ion in between two helixes associated with the 7 oxygens in them. If we consider PEO to behave as an open-chain analogue of crown ethers, then the model

proposed here is consistent. That is, what we appear to have are two types of complexes, the first consisting of single helical turns and single cations and the second a sandwich-like complex of two helical turns with a single cation in the middle. Such 1:2, cation to crown ether, complexes are well-known[8] and we believe that something similar is occurring here. For other polymer/salt systems reported in the literature a single crystalline complex has been observed at various ratios including 4:1,[9] 3:1,[10] and also 3.5:1 as observed here. (The 3.5:1 concentration for the crystalline complex was reported by Berthier et al. and was assumed from NMR data.)[3]

Some evidence for additional phases has been presented by Neat et al., who have isolated at least three distinguishable spherulite types in the PEO/$LiClO_4$ system.[11] Additional support for a second phase has recently been reported.[12] In that study the authors also looked at PEO/$LiClO_4$ by DSC and concluded that two distinct stoichiometric crystalline complexes, 3:1 and 6:1, were found together over a range of concentrations in the phase diagram. Similar data taken in another laboratory were interpreted as a eutectic in the phase diagram.[13] Our own work with a different salt system is consistent with the interpretation of a mixture of two crystalline complexes being present in the phase diagram. Also, recent work on the same PEO/$LiCF_3SO_3$ complex seems to be at odds with our results.[14] These authors do not find evidence for more than one crystalline complex in PEO/$LiCF_3SO_3$. However, in the same paper evidence for multiple intermediate crystalline complexes in the $LiClO_4$ and $LiAsF_6$ systems is presented. Clearly, the interpretation of phase data is not one that is yet uniformly undertaken.

X-ray diffraction data coupled with DSC data, here, indicate two crystalline phases in the PEO/$LiCF_3SO_3$ samples. It is observed that the two crystalline phases do not exist only at one concentration but occur over a range. The highest concentrations center around the 3.5:1 composition for phase A material and near 7:1 for phase B material. These phases coexist along the whole spectrum of samples prepared for the PEO/$LiCF_3SO_3$ study. Their relative amounts and degree of crystallinity change with increasing salt concentration, and therefore one could envision this fluctuation as a simple rearrangement of the Li-associated polymer loops. In contrast, for the PEO/$LiBF_4$ system, a single crystalline complex is observed over a range of stoichiometries but appears in highest concentration between 3:1 and 4:1. For both salt complexes a very small amount of free crystalline PEO is indicated at the 4:1 ratio. At the 3:1 composition some small differences exist in peak character at low angles, indicating the presence of some amorphous complex material.

At high salt concentrations, the difference between the two salt systems is notable. For the $PEO_2(LiBF_4)$ sample, reflections for free salt are observed. In the PEO/$LiCF_3SO_3$ system, however, the presence of free salt is only indicated at the more concentrated level of 1:1. We take this to mean that either the polymer–salt mixture consists mostly of a single crystalline complex or that much of the mixture has become amorphous. Concentrations beyond the 1:1 limit were excluded from the study because these samples have been shown to exhibit poor conductivity and are mechanically brittle.[3]

Figures 3 and 4 show the DSC data of the various $LiBF_4$ and $LiCF_3SO_3$ concentrations dissolved in the polymer. Pure poly(ethylene oxide) (mol wt 5×10^6) in film form melts at ~69 °C. All DSC temperatures are given as the peak maxima. $LiBF_4$ decomposes at ~300 °C. $LiCF_3SO_3$ is stable within the temperature region of interest. Small

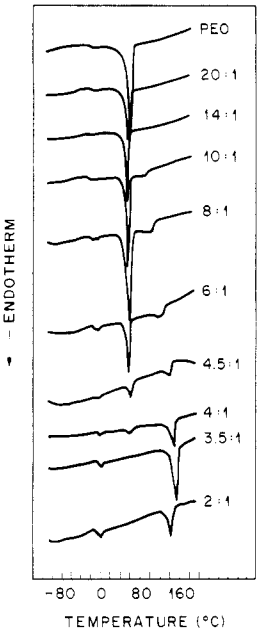

Figure 3. DSC traces of $PEO_x(LiBF_4)$. Ratios of polymer/salt are indicated.

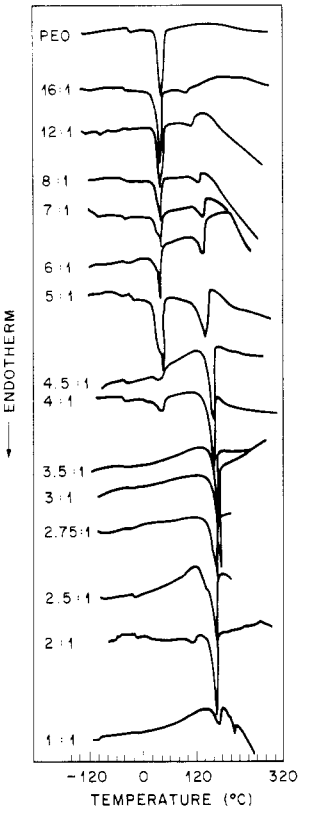

Figure 4. DSC traces of $PEO_x(LiCF_3SO_3)$.

peaks observed in all DSC scans centered around 0 °C are attributed to melting of low molecular weight PEO oligomers, present at impurities.

Addition of small amounts of $LiBF_4$ up to ~15:1 composition results in very little change in the DSC trace except for a slight melting point depression (~3 °C). This is not observed in the $LiCF_3SO_3$ system. When the salt concentration is increased, two endotherms are detected by the DSC, for the PEO/$LiBF_4$ system, one attributed to the melting of free crystalline PEO and the other to the melting/dissolution of the complex crystalline phase. In addition, the DSC data show, as the PEO peak at ~69 °C

decreases in magnitude, the higher temperature transition increases intensity and occurs at higher temperature at the peak maxima. At the ratio of 3.5:1 all traces of the endotherm associated with pure PEO disappears, leaving a single melting endotherm of the fully complexed polymer/salt phase.

Data for the PEO/$LiCF_3SO_3$ is more complicated. In general, the trend is the same as that of $LiBF_4$ samples. Two main endotherms characteristic of crystalline PEO melting and a crystalline complex melting are demonstrated. However, a shoulder appears at ~60 °C near the PEO melting endotherm. This may be additional evidence for the second crystalline phase (phase B) observed by X-ray diffraction.

Both DSC and X-ray data indicate the 7:1 composition contains the largest amount of phase B. Therefore, the stoichiometry of this phase is inferred near 7:1. This phase also may exist over a range of stoichiometry as does the 3.5:1 phase. Additional experiments to confirm this have not been completed.

Optical polarizing microscopy has been used by Stainer[15] and others to confirm DSC results by indicating changes in samples as they change phases from crystalline to amorphous. Similar experiments on both salt systems studied here, however, provide little additional information. Samples show that the defined spherulites undergo only one uniform transformation to the amorphous state at the upper transition temperature. PEO melting and spherulite changes, if any, are not observed. The probable reason is the high rate of dissolution of the salt into PEO. As the PEO crystalline regions approach their melting point, the salt rapidly redistributes itself from surrounding amorphous regions, leaving no evidence detectable by the microscope. To prove that the low-temperature transition then could truly be attributed to PEO melting, an X-ray pattern at 75 °C was taken which distinctly shows the disappearance of only the crystalline PEO peaks. This is shown for the 6:1 composition of the $LiBF_4$ salt in Figure 1.

Investigation of DSC traces on either side of the 3.5:1 concentration supports the conclusion obtained from X-ray data, that the fully complexed polymer covers a range of stoichiometries. At 4:1, only a small amount of pure PEO remains, and at 3.0:1 the DSC trace is identical with that of 3.5:1. Therefore it appears that the amount of each phase with a single unique stoichiometry is present in varying amounts, and this is true for both $LiCF_3SO_3$ and $LiBF_4$ complexes.

At higher than 3:1 polymer/salt concentrations, the DSC data indicate more than one phase is present for both salt systems. A small melting point depression (~2 °C), indicative of excess salt, is apparent beginning with $PEO_{2.75}(LiCF_3SO_3)$. The main endotherm exhibits an even lower temperature at the peak maxima for $PEO_{2.5}(LiCF_3SO_3)$, and a shoulder appears. This trend then continues with the 2:1 sample showing both endotherms (now distinct) at lower temperatures. Samples prepared in this high concentration regime (especially 1:1 and 2:1) did not give reproducible DSC scans, and therefore the possibility of a single phase material as suggested by the X-ray data at $PEO_2(LiCF_3SO_3)$ is not likely. The PEO/$LiBF_4$ system also shows a melting point depression in the 2:1 sample; however, X-ray data clearly shows the presence of free salt at this concentration, and therefore higher salt concentration samples were not prepared. DSC data of polymer films containing each salt are similar by direct comparison. Small differences exist in the form of shoulders near the low-temperature endotherm for PEO

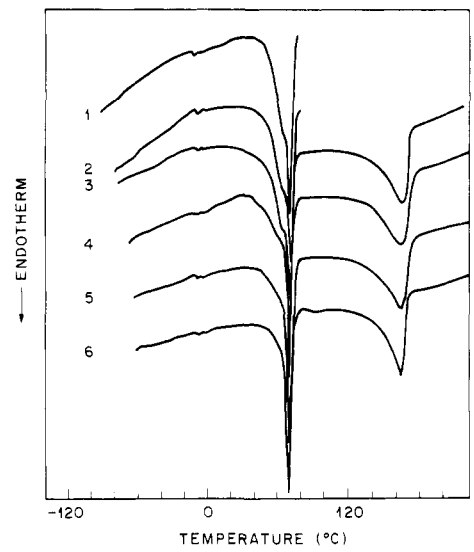

Figure 5. Comparison of DSC data for the $PEO_7(LiCF_3SO_3)$ sample, after heating to various temperature limits.

melting. Two primary endothermic events are apparent in each case. Both salts show a progressive change from a complex phase system to one phase, the single phase appearing over a range between 3:1 and 4:1. Beyond this region, excess salt is present and the samples are inhomogeneous. The DSC scans were repeated for each of the polymer samples. The $LiBF_4$ system consistently exhibited reproducible data. This apparent phase stability is an important asset when considering the potential use in a rechargeable battery cell. The $LiCF_3SO_3$ system did not display the same stability. Other salt complexes with PEO reported in the literature have also shown evidence for hysteresis.[16] The largest changes noted in the DSC data for second scans occur in the stoichiometry range $PEO_{12}(LiCF_3SO_3)$ to $PEO_5(LiCF_3SO_3)$. In this region an endothermic shoulder is seen at ~61–62 °C.

As already mentioned this may be attributed to phase B material or a eutectic composition. When the same samples are heated a second time, this shoulder would sometimes repeat, but not consistently. Figure 5 shows the results for $PEO_7(LiCF_3SO_3)$ after the same sample is heated to various temperatures. Scan 1 shows the first heating to 80 °C and scan 2, the second heating. Scans 3, 4, and 5 are first, second, and third heating runs to 220 °C, respectively. Scan 6 is the same sample after fast quenching to ~−130 °C. When the sample is heated to 220 °C for the second time, the size of the shoulder diminishes; however, only upon quenching from 250 at 60 °C/min does the shoulder disappear. This is consistent with an additional phase, as proposed.

To gain more information about what structural or phase changes might be characterized, X-ray diffraction data were taken after the samples were heated to ~220 °C and slowly cooled. Figure 6 presents X-ray diffraction data for several stoichiometries of the $LiCF_3SO_3$ system. Most of the samples produced repeatable patterns. The 7:1 sample showed an obvious shift in intensities between the peaks at 2θ values of 20.53 and 21.45. The 7:1 sample looks much the same as the 3.5:1 sample after recrystallization except for the presence of uncomplexed PEO. Curiously, the 2:1 composition produced a pattern identical with that of 3.5:1 after heating and slow cooling, except for one peak. This extra peak does not correspond to either pure PEO or $LiCF_3SO_3$. In addition this peak grows in intensity after the heating/slow cooling process is repeated once more. The DSC pattern of 2:1 and 1:1 con-

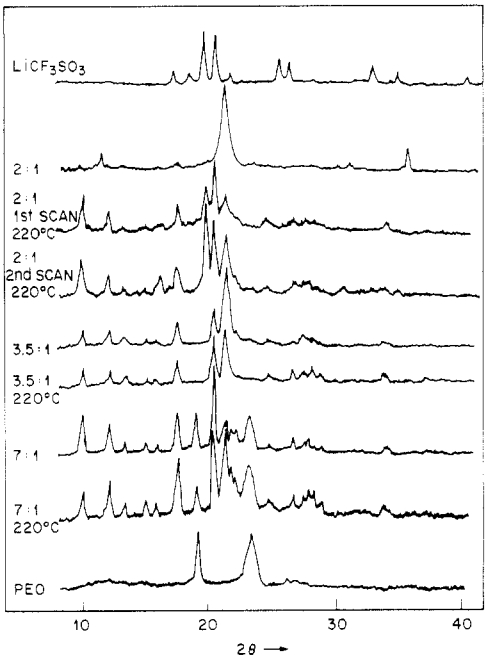

Figure 6. X-ray diffraction data for several stoichiometries of the $LiCF_3SO_3$ system after recrystallization.

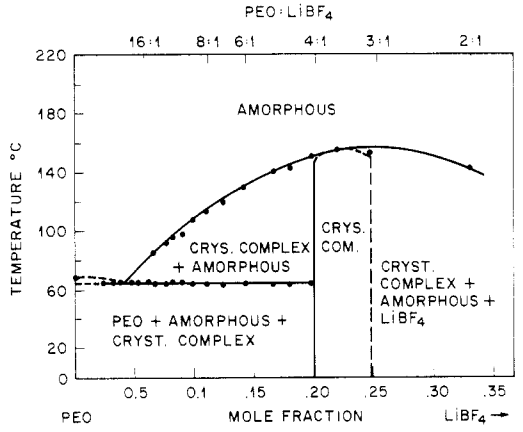

Figure 7. Pseudophase diagram of the $PEO_x(LiBF_4)$ system.

centrations on second heating cycles show large changes. This is expected because of the availability of excess salt producing nonuniformly distributed crystalline regions.

Despite the more complicated data obtained from the $PEO/LiCF_3SO_3$ system, both salt systems display similar trends as already mentioned. This becomes clear by looking at the PPD (in Figures 7 and 8) which we have constructed from our DSC and X-ray analysis. Temperature-controlled optical microscopy was used to study the spherulites of both salt complexes. The spherulites are composed of both amorphous and crystalline regions. Characterization of the amorphous regions is not possible from the data contained in this report. The phase diagrams, therefore, reflect only the effects of the crystalline portions of both PEO and the PEO/salt complex. For the $PEO/LiBF_4$ system, at temperatures below the melting point of PEO and with salt concentrations lower than the 3.5:1 level, both PEO (crystalline and amorphous) and the crystalline complex (crystalline and amorphous) coexist in solid form. At these same compositions but above ~ 65–68 °C, the crystalline complex and an amorphous phase are present, crystalline PEO having melted. Within a range of stoichiometries between ~3.0:1 and 4.0:1 a single phase is formed and beyond this concentration at 2:1 the crystalline complex coexists with free salt.

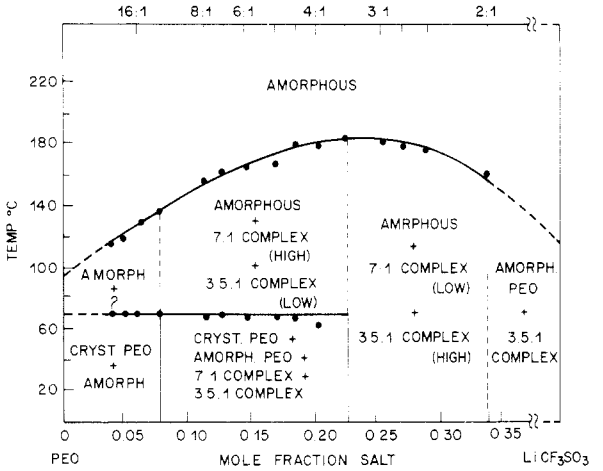

Figure 8. Pseudophase diagram of the $PEO_x(LiCF_3SO_3)$ system.

For $LiCF_3SO_3$ free salt is observed only at the 1:1 level. As the salt concentration is lowered, the crystalline complex phase A is first observed along with some amorphous material. The phase diagram between 1:1 and 3:1 is speculative, and a mixture of inhomogeneous phases may exist hence the dotted lines. From X-ray and DSC data contained in this report, the range of stoichiometries between 3:1 and 4:1 contains mainly the 3.5:1 crystalline complex (phase A) with phase B present in very small quantities. Below 4:1, phase B is predominant, but phases A and B do coexist, together with crystalline PEO and amorphous material. Upon recrystallization of the 7:1 sample concentration (by heating to 220 °C and slow cooling) the ratios of the 3.5:1 phase A and 7:1 phase B change, with an increase in the phase A peak intensity, indicating phase A is likely the most stable phase. This illustrates the problem of expressing the polymer/salt systems in phase diagram form. The $LiCF_3SO_3$ system is particularly difficult to represent in this way because of the apparent nonequilibrium conditions in the system. Nevertheless, in Figure 8 we have attempted to express the various phase relationships as well as possible, given the constraints of a two-dimensional drawing. Phase areas of controversy, or of incomplete data, but most particularly regions of varying concentrations of phases have been designated with broken lines. In contrast, Figure 7 for the $LiBF_4$ system is much simpler. Complications due to multiple crystalline phases do not exist.

To date few phase diagrams on the PEO salt complex systems have been published. Stainer et al.[15] investigated ammonium salt PEO complexes and presented an approximate phase diagram for PEO/NH_4SCN. That system was studied mainly for the transport information obtained about proton-containing species in a polymer/salt complex. A binary phase diagram for the PEO/NaSCN system[17] was shown to account for the observed phase behavior and was used to model both the temperature and concentration dependence of the conductivity. The phase diagram for $PEO/LiCF_3SO_3$ has been studied by several groups including, Weston and Steele,[18,19] Sorensen and Jacobsen,[20] and Minier, Berthier, et al.[3] The most complete phase diagram has been reported by Minier, Berthier, et al. A comparison between data presented here and that reported by these workers shows good agreement despite the fact that Minier annealed his samples (207 °C) and used a lower molecular weight poly(ethylene oxide). The greatest difference between the two studies lies in the interpretation of the stoichiometry of the single phase crystalline complex. Our study suggests the presence of two separate crystalline phases (of distinct stoichiometries), each of

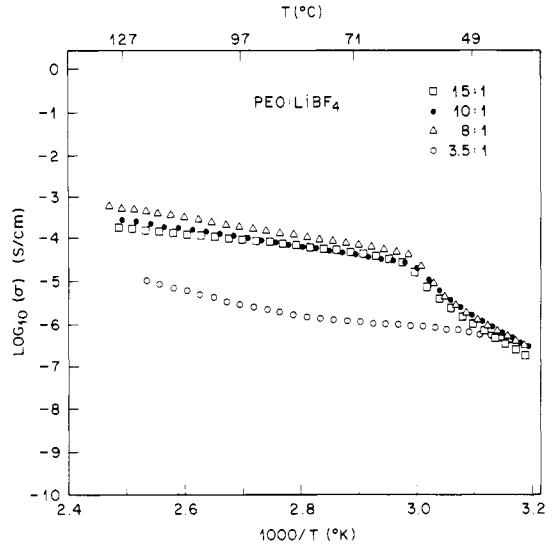

Figure 9. Plot of log σ versus $1/T$ for various stoichiometries of $PEO_x(LiBF_4)$.

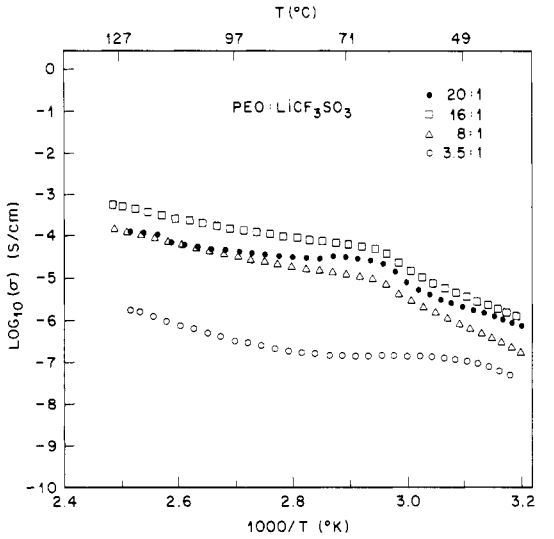

Figure 10. Plot of log σ versus $1/T$ for representative stoichiometries of $PEO_x(LiCF_3SO_3)$.

which may exist over a fairly wide polymer/salt composition range. Minier and Berthier et al.[3] inferred a fixed stoichiometry of 3.5 from an NMR study of PEO/$LiClO_4$ and PEO/$LiAsF_6$. These workers did not investigate the higher salt concentration region of the PEO/$LiCF_3SO_3$ system as is noted here, but as discussed above, they did find multiple intermediate crystalline complexes, except in the case of $LiCF_3SO_3$. In this latter case evidence was also presented for a eutectic at very low salt concentrations. Our data do not go to low enough concentrations to be sure of this eutectic.

Another controversial point regarding polymer/salt systems in general in the possibility of a eutectic compound at low salt concentrations. For the PEO/NH_4SCN system a eutectic is apparent at 8:1 with a melting point of 42 °C. A slight melting point depression is observed for PEO/$LiBF_4$ salt concentrations below 40:1. This may be evidence for a similar eutectic with a very low Li^+ salt concentration (<40:1, Figure 7). Evidence for a eutectic is not conclusive from the data obtained here for $LiCF_3SO_3$, although some demonstration of its existence has been presented by Sorensen et al.[20] and Robitaille et al.[14]

Arrhenius plots for conductivity data are illustrated in Figures 9 and 10. The curves can be associated with two approximately straight line regions, each exhibiting Arrhenius-type behavior. Activation energies for each region are reported for a representative sample of stoichiometries in Table I. Activation energies range between 0.48 and 0.27 eV for the high-temperature regime, and between 0.90 and 1.64 eV for the low-temperature regime (below 60 °C). The higher temperature data show a clear trend toward lower activation energies for transport at lower salt concentrations. No trend is apparent in the lower temperature data. The plots show a knee in the data at the approximate melting point of pure PEO (66–68 °C). Similar behavior has been noted in previous reports.[4,21,4] The highest conductivities in all samples occur consistently at temperatures above the melting point of the crystalline complex, indicating the totally amorphous state is responsible for ionic conduction. This has been established by several groups.[22-24] There have been a number of recent efforts to prepare polymers that will form low T_g fully amorphous complexes with various salts. These rely on the substitution of linear polymers, for example, polymethacrylates[25] and polyphosphazenes,[26] with short oxyethylene units. Such polymers form complexes with conductivities equal to or surpassing those of analogous PEO complexes.

Table I
Conduction Activation Energies of $PEO_x(LiBF_4)$ and $PEO_x(LiCF_3SO_3)$

	PEO:SALT	ACTIVATION ENERGY (eV) LOW TEMP. REGION	ACTIVATION ENERGY (eV) HIGH TEMP. REGION
$LiBF_4$	2:1	1.36	0.48
	4:1	0.98	0.34
	4.5:1	1.64	0.33
	6:1	1.09	0.29
	8:1	1.42	0.27
	10:1	1.47	0.29
	15:1	1.57	0.29
$LiCF_3SO_3$	4.0:1	1.07	0.39
	4.5:1	0.90	0.37
	5:1	1.36	0.33
	6:1	1.27	0.35
	8:1	1.26	0.33
	12:1	0.94	0.29
	16:1	1.04	0.28

Of the two complexes studied here, $PEO_8(LiBF_4)$ shows the highest conductivity (9×10^{-4} S/cm at ~125 °C), although the $PEO_{16}(LiCF_3SO_3)$ sample has a conductivity value of the same order of magnitude (7×10^{-4} S/cm at 125 °C). For all temperatures the precision in the measurement of conductivity is approximately log 0.2 (S/cm). Throughout the temperature range (40–130 °C) the samples in general exhibit lower conductivities at higher salt concentrations. Experimental data were reproducible upon second heatings for both salt systems. One exception to this was the high salt concentration sample of the PEO/$LiCF_3SO_3$ system.

A study of a large number of different lithium salts was published by Rietman et al.,[4] to attempt a correlation between anion character and improved conductivity. Essentially no direct trends were established other than a noted decrease in conductivity for oxygen-containing anions. This is presumably due to the effect of hydrogen bonding with residual water, which essentially removes the anion from contributing to the charge transport scheme. In early work in this field anions were not considered valuable contributors to the ionic conductivity, however it is now widely accepted that for most polymer/salt systems studied, both anions and cations are mobile and

both have a large affect on the total conductivity.[3,19,27-29]

Conclusions

The PPD for both PEO_x·$LiBF_4$ and PEO_x·$LiCF_3SO_3$ demonstrate very similar phase relations over the majority of the concentration range studied. The PEO/$LiCF_3SO_3$ system is more complicated, and the data illustrate two separate crystalline complex phases. Some difference are noted at high salt concentrations (2:1) between the two systems, but reproducible data were not obtained and therefore nonequilibrium sample conditions must predominate.

Through examination of a large number of samples, a stoichiometry range between 3:1 and 4:1 was established for the fully complexed crystalline compound in the $LiBF_4$ polymer/salt scheme.

The combination of conductivity results with the PPD diagram information indicates the conductivity is both temperature- and concentration-dependent. In addition, the highest conductivity samples were obtained when an amorphous dilute salt phase was dominant. This exists at temperatures above 65 °C and in different concentrations for each salt. The highest conductivity for PEO_x·$LiBF_4$ was obtained at $x = 8$ and for PEO_x·$LiCF_3SO_3$ at $x = 16$.

Although the conductivity data have been plotted in the form of log σ vs. $1000/T$, we do not believe one conductivity model describes the data more accurately than any other. This is due to the changing ratio and compositions of the amorphous and crystalline phases over much of the temperature range studied in the polymer/salt systems. Only above the temperature where the entire polymer film is amorphous would a fit of the data to one particular form be appropriate. Interpretation of the conductivity in this region is most often made in terms of the Vogel–Tamman–Fulcher equation[30] for ionic glasses or the more detailed model of the free volume theory of Cohen and Turnbull.[31,32]

This study establishes the general trend of phases present in PEO/Li^+ systems, however, a closer look into the makeup of the amorphous regions is essential for a full understanding of the transport mechanism.

Acknowledgment. We wish to thank Prof. R. D. Andrews (Steven's Institute of Technology, Hoboken, NJ) for contributions involving a portion of this work which was completed as part of a Master's Degree program. A. J. Lovinger is thanked for the use of his optical microscopy equipment and for helpful discussions.

Registry No. $LiBF_4$, 14283-07-9; $LiCF_3SO_3$, 33454-82-9.

References and Notes

(1) Fenton, B. E.; Parker, J. M.; Wright, P. V. *Polymer* **1973**, *14*, 589.
(2) Armand, M.; Chabango, J. M.; Duclot, M. *Fast Ion Transport in Solids*; Vashishta, P., Mundy, J. N., Shenoy, G. K., North-Holland: New York, 1979; p 131.
(3) Minier, M.; Berthier, C.; Gorecki, W. J. *J. Phys. (Les Ulis, Fr.)* **1984**, *45*, 739.
(4) Rietman, E. A.; Kaplan, M. L.; Cava, R. J. *Solid State Ionics* **1985**, *17*, 67.
(5) North, J. M.; Sequeira, C.; Hooper, A.; Tofield, B. C. International Meeting on Li Batteries, Abstract No. 32, Rome, April 1982.
(6) Armstrong, R. D.; Clarke, M. D. *Solid State Ionics* **1984**, *11*, 305.
(7) Takahashi, Y.; Tadokoro, H. *Macromolecules* **1973**, *6*, 672.
(8) Poonia, N. S. In *Progress in Macrocyclic Chemistry*, Izatt, R. M., Christensen, J. J., Eds.; Wiley-Interscience: New York, 1979; Vol. I, p 115 ff.
(9) Hibma, T. *Solid State Ionics* **1983**, *9*, *10*, 1101.
(10) Catlow, C. R. A.; Chadwick, A. V.; Greaves, G. N.; Moroney, L. M.; Worboys, M. R. *Solid State Ionics*, **1983**, *9*, *10*, 1107.
(11) Neat, R. J.; Hooper, A.; Glass, M. D.; Linford, R. G. In Proceedings of the 6th Riso International Symposium on Metallurgy and Material Science; Foulsen, F. W., Anderson, N. H., Clausen, K., Skaarup, S., Sorensen, O. T., Eds.; September 1985, p 341.
(12) Gorecki, W.; Andreani, R.; Berthier, C.; Armand, M.; Mali, M.; Roos, D.; Brinkman, D. *Solid State Ionics* **1986**, *18*, *19*, 295.
(13) Ferloni, P.; Chiodelli, G.; Magistris, A.; Sanesi, M. *Solid State Ionics* **1986**, *18*, *19*, 265.
(14) Robitaille, C. D.; Fauteux, D. *J. Electrochem. Soc.*, **1986**, *133*, 315.
(15) Stainer, M.; Hardy, C. L.; Whitmore, D. H.; Shiriver, D. F. *J. Electrochem. Soc.* **1984**, *131*, 784.
(16) Chiang, C. K.; Davis, G. T.; Harding, C. A.; Aarons, J. *Solid State Ionics* **1983**, *9*, *10*, 1121.
(17) Lee, Y. L.; Crist, B. *J. Appl. Phys.* **1986**, *60*, 2683.
(18) Weston, J. E.; Steele, B. C. H. *Solid State Ionics* **1981**, *2*, 347.
(19) Weston, J. E.; Steel, B. C. H. *Solid State Ionics* **1982**, *7*, 81.
(20) Sorensen, P. R.; Jacobsen, T. *Polym. Bull.* **1983**, *9*, 47.
(21) Papke, B. L.; Dupon, R.; Ratner, M. A.; Shriver, D. F. *Solid State Ionics* **1981**, *5*, 685.
(22) Berthier, C.; Gorecki, W.; Minier, M.; Armand, M. B.; Chabagno, J. M.; Rigand, P. *Solid State Ionics* **1983**, *11*, 91.
(23) Minier, M.; Berthier, C.; Gorecki, W. *Solid State Ionics* **1983**, *9*, *10*, 1125.
(24) Button, D. P.; Mason, L. S.; Tuller, H. L.; Uhlmann, D. R. *Solid State Ionics* **1983**, *9*, *10*, 585.
(25) Xia, D. W.; Stoltz, D.; Smid, J. *Solid State Ionics* **1984**, *14*, 221.
(26) Blonsky, P. M.; Shriver, D. F.; Austin, P.; Allcock, H. R. *Solid State Ionics* **1986**, *18*, *19*, 258.
(27) Payne, D. R.; Wright, P. V. *Polymer* **1982**, *23*, 690.
(28) Sorensen, P. R.; Jacobsen, T. *Electrochem. Acta* **1982**, *27*, 167.
(29) Hardy, L. C.; Shriver, D. F. *J. Am. Chem. Soc.* **1985**, *107*, 3823.
(30) Fulcher, G. S. *J. Am. Ceram. Soc.* **1925**, *8*, 339.
(31) Cohen, M. H.; Turnbull, D. *J. Chem. Phys.* **1961**, *34*, 120.
(32) Cohen, M. H.; Turnbull, D. *J. Chem. Phys.* **1970**, *52*, 3038.